

TECHNICAL BACKGROUND FOR “A PRECISION MEDICINE APPROACH TO DEVELOP AND INTERNALLY VALIDATE OPTIMAL EXERCISE AND WEIGHT LOSS TREATMENTS FOR OVERWEIGHT AND OBESE ADULTS WITH KNEE OSTEOARTHRITIS”

Data from the Intensive Diet and Exercise for Arthritis (IDEA) Trial

Xiaotong Jiang, BA¹, Amanda E. Nelson, MD MSCR², Rebecca J. Cleveland, PhD², Daniel P. Beavers, PhD³, Todd A. Schwartz, DrPH¹, Liubov Arbeeva, MS², Carolina Alvarez, MS², Leigh F. Callahan, PhD², Stephen Messier, PhD⁴, Richard Loeser, MD^{2*}, Michael R. Kosorok, PhD¹

¹Department of Biostatistics, University of North Carolina, Chapel Hill, NC

²Division of Rheumatology, Allergy and Immunology and the Thurston Arthritis Research Center, University of North Carolina, Chapel Hill, NC

³Department of Biostatistics and Data Science, Wake Forest School of Medicine, Winston-Salem, NC

⁴Department of Health and Exercise Science, Wake Forest University, Winston-Salem, NC

***CORRESPONDING AUTHOR:**

Richard F. Loeser, MD

Division of Rheumatology, Allergy and Immunology

Thurston Arthritis Research Center

3300 Thurston Building, CB#7280

University of North Carolina, Chapel Hill, NC

E-mail: richard_loeser@med.unc.edu

KEYWORDS: Knee Osteoarthritis, Precision Medicine, Machine Learning

FUNDING SOURCE

The IDEA trial was funded by a grant from NIAMS (R01 AR052528). Support for the precision medicine analysis was provided by NIAMS grant P60 AR064166, P30 AR072580, P01 CA142538, and UL1 TR002489.

Methods

Data Cleaning. We performed extensive data cleaning for the baseline covariates in the raw IDEA trial data. First, marital status was originally classified into six categories and we combined them into two categories, where 1 stands for presently married and in a married-like relationship and 0 stands for never married, divorced/separated, and widowed. Second, three questions, “How many falls have resulted in injury, minimal medical attention, and hospitalized/bedridden?”, had -1 values because the patient answered “no” to a previous question “Over the past 6 months, how many times you have fallen on the ground?”. We converted all -1 values to 0’s as no falls have resulted in the three conditions since the patient had not fallen in the past six months. Third, we reordered ordinal variables such as education, alcohol, and thinking of falling (i.e. “how often do you think about falling”) so they were all ordered from never/low to current/high. Binary variables were converted from values of 1 or 2 to values of 0 or 1. Fourth, two variables, “number of falls resulted in hospitalization” and “pacemaker condition” were excluded from the cleaned data because they have no or only a few cases when almost all other patients answered “no”. With too few cases, these would not spread evenly across training and validation sets, which could generate unreliable estimates and predictions. Lastly, we excluded follow up data at 6th month, kept baseline and 18th month data only, and reshaped the raw data from a long to a wide format.

Dimension Reduction. The original IDEA analysis includes 76 variables, all measured at baseline, including standard sociodemographic factors, anthropomorphic measures, measures related to co-morbidities, self-reported measures of pain and function, as well as quality of life, physical performance measures including gait and strength analysis, and blood levels of inflammatory markers including IL-6 at baseline and C-reactive protein (CRP) at baseline. As part of the preprocessing, we performed dimensionality reduction to remove unimportant or highly correlated covariates. Among patients with complete outcome measures, we applied a random forests model to each outcome separately and acquired variable importance measures of the covariates (see Supplemental Table 2 for a list of brief explanations of statistical terms and abbreviations used throughout this supplemental material). Random forests (RF) are a suitable dimension reduction tool because they can examine both the marginal and multivariate predictive performance of predictors. The categorical variables in our input data have two to six categories, which are comparable scales for the importance scores of RF to be valid. A variable was considered to be “statistically important” if it was among the top 10 most important variables for at least three of the outcomes that RF was modeled on, or the value of its scaled mean squared error (MSE) rate was at least 9. We observed that more predictors have low importance scores compared to those with high scores. Thus, our two criteria filtered out noisy, non-influential variables and maintained influential variables that are either important to many outcomes or extremely important to a single outcome. A variable was considered to be “clinically important” if it is patient-reported or a test result that could be obtained in medical settings (such as blood levels of IL-6 or DXA). Thus, we avoided using the variables generated by gait analysis since

this would require patients to be assessed in a gait lab which would not be available in most medical settings. As a result, we included 15 covariates in input Data 1 and 17 baseline covariates in input Data 2 (Table 1) because they were missing less than 15% of the values and were considered to be both clinically and statistically important.

Missing Data and Imputation. In addition to the multiple imputation analysis conducted in the original IDEA study, we looked into the missingness pattern in the preprocessed Input Data 2 (with 7 outcomes) from two perspectives. We first performed logistic regression modeling for raw X covariates on the missingness of each outcome (0/1), and none of the X covariates was found to be significant. We also calculated Spearman correlation coefficients between the original data and the corresponding indicator data of 0/1's (where 0 means the value is not missing, and 1 means it is missing). Mixing the covariates and outcomes together, we randomly sampled five variables at a time (to maintain the size of the square matrix) but repeated this random sampling 15 times. Most pairwise correlations between the original data and missingness indicator data were less than 0.2, except around 1 to 6 occasional moderate correlations observed per sample, which was partially due to moderate correlations between the two original variables. After we confirmed that there were no obvious missing data problems, imputation was conducted on covariates missing in less than 15% of the participants because too many missing data points would lead to biases and potentially poorly imputed values. The imputation process was completely unsupervised (using only X-variables) because more biases would be introduced if outcomes were involved at this stage. The algorithm missForest fit our study because it did not require assumptions about the data distribution, can be applied to high-dimensional mixed-type data of unequal scales, utilized out-of-bag imputation error estimates to avoid CV, and outperformed other popular imputation methods such as multiple imputation by chained equations (MICE) (1).

Choice of Models. Table 2 shows all the models we considered in the clinical data analysis. Penalized regression is a linear regression model that penalizes high-dimensional data in the model by shrinking the coefficients. This kind of model reduces variance of coefficients and automatically reduces dimensions while making predictions as a regular linear model. We chose three kinds of penalty terms (lasso, ridge, and elastic net) that differ in terms of the amount of shrinkage determined by a penalty parameter: lasso (M1) forces coefficients to be exactly zero with an absolute value penalty and ridge (M2) forces the coefficients to be close to zero with a squared term penalty, whereas elastic net (M3) with parameter $\alpha = 0.5$ is an even mix of lasso and ridge. Kernel ridge regression (KRR) (M4) is a ridge regression method that directly computes kernel functions to make predictions and the Gaussian kernel extends the regression model to a more flexible, non-linear space (2). We chose RF for individual outcomes (M5) and weighted multiple outcomes (M6) because RF is a common prediction method that reduces overfitting and variance significantly by aggregating a group of independent individual classifiers. RF also takes into account variable interactions sequentially with its tree structure without user-specification. RLT (M7) is similar to RF as they are both tree-based methods, but it has two attractive properties: RLTs can eliminate noise

variables with a built-in muting procedure and implements reinforcement learning to select variables at each node that improve outcomes in the long run (3).

Although RF usually generates good predictions, it is often considered a “black-box” because it lacks the interpretability when averaging over many individual trees. In contrast, list-based DTRs estimate optimal treatment regimens with a sequence of decision rules which can be easily interpreted as lists, a set of “if-then” statements (4). The list-based models first require predictions of the potential outcome under all treatment options before generating interpretable lists. We embedded four models to make such predictions: KRR, RF, super learning, and elastic net with $\alpha = 0.5$. Super learning (SL) is a recent semi-parametric ensemble method (5,6) that learns the optimal decision rules by combining candidate learners with weights instead of selecting only one optimal model and is applicable to dynamic treatment regimens with multiple time points. The candidate learners are BART, elastic net, KRR, lasso, RF, RLT, and ridge. We implemented super learning algorithm with simulated annealing as the meta learner that learns the weights of the seven base learners and optimizes the super learning model. Simulated annealing is a numerical optimization method that speeds up optimization by finding the approximate global optima (as opposed to the exact global optima) without getting stuck in local optima (7). Our implementation can be found on our GitHub repository (<https://github.com/phoebejiang/pmoa>). The default number of list nodes, which is the maximum number of “if-then” statements, is 10. The higher the number of nodes, the more complicated it will be for interpretation of the estimated list of statements, so we also considered simpler lists with 2, 3, and 5 nodes for list with KRR, SL, and RF (M8 - M19). The majority of the candidate models are list-based DTRs because of their interpretability and flexibility in accepting multiple treatments and different types of embedded models for outcome prediction. Note that a list with 1 node is equivalent to a ZOM because it always assigns patients to the same group.

Residual weighted learning (RWL) models use outcome residualization to improve on outcome-weighted learning (OWL), a policy learning model that optimizes clinical outcomes directly (8,9). Using residuals instead of the original outcomes allows RWL to handle various types of outcomes and any shifts in the outcomes. We chose three kernels to learn both linear and nonlinear decision rules: linear kernel (M21), 2nd order polynomial kernel (M22), and 3rd order polynomial kernels (M23). Gaussian kernels can be more flexible but were not considered due to the burden of extensive computation times and interpretational difficulties. The current RWL algorithm can only deal with two treatments, and we generalized the model to three treatments by performing a two-stage procedure: 1) First fit RWL to the control group E versus D and D+E group combined; 2) Then fit RWL again to only patients whose optimal group was predicted to be in the D and D+E combined group to further distinguish the optimal group as D versus D+E. Finally, Bayesian Additive Regression Trees (BART) (10) is an ensemble method similar to the idea of RF, but each tree in the ensemble is regularized by a prior distribution, and predictions are made from resampling from the posterior distribution. We included this nonparametric model for its flexibility in accepting various data types and its direct inference on estimation precision.

The following R packages were used to run the models mentioned above: “glmnet” (11) for penalized regression models (M1-3), “listdtr” for KRR and list-based models (M4, M8-16) (4), “randomForest” (12) for RF models (M5-6), “RLT” (3) for the RLT (M7) model,

“DynTxRegime” (13) for RWL models (M21-23), and “BART” (14) for the Bayesian model (M24).

Value Function. The true value function is the expected reward of a potential outcome under ITR d and is defined as

$$V_o(d) = E[Y^d] = E \left[Y \frac{1\{A = d(\mathbf{X})\}}{P(A|\mathbf{X})} \right]$$

where $\mathbf{X} \in \mathcal{X} \subseteq \mathbb{R}^p$ represent patient covariates with p dimensions, $A \in \mathcal{A}$ is treatment group, $Y \in \mathcal{Y} \subseteq \mathbb{R}$ is the clinical outcome of interest, and d is the decision rule that maps patient information to a treatment (15). The true value function is often estimated empirically by

$$\hat{V}(d) = \frac{\sum_{i=1}^n Y_i 1\{A_i = d(\mathbf{X}_i)\} / P(A_i|\mathbf{X}_i)}{\sum_{i=1}^n 1\{A_i = d(\mathbf{X}_i)\} / P(A_i|\mathbf{X}_i)},$$

which can be deemed as a weighted combination of individual outcomes.

The Jackknife. The “leave-one-out” jackknife idea was first brought up by Quenouille (16) and Tukey (17) to reduce estimation bias, which later inspired the bootstrap resampling methods. Back in 1995, Kohavi (18) claimed that jackknife “has smaller (pessimistic) bias but larger variance than leave-more-out CV”. This statement is influential, but rather broad and debatable. There has been much literature pertaining to the performance of jackknife estimators that is more specific and substantiated. In least square linear regressions, Burman (19) showed that jackknife (also referred to as ordinary CV) estimates reached the lowest biases and variances among other k-fold CV estimates for simulated samples of 12 and 24. A recent publication by Zhang and Yang (20) in 2015 argued that the jackknife is “typically the best or among the best for a fixed model or a very stable modeling procedures in both bias and variance, or quite close to the best in mean squared error (MSE) for a more unstable procedure.”

The jackknife method was chosen in this article because it requires weak assumptions, which are typical assumptions such as independent and identically distributed observations (this can be more representative of future data). Given reasonable sample sizes like that in this paper, the jackknife is relatively easy to implement because it loops through each patient once and only once without the need of repetitions. As for bias and variance trade-off, we took into account the correlation among the training sets when calculating variance estimates and test statistics of jackknife estimators, as shown below and in the next section. Furthermore, we show that our jackknife estimators retain algorithmic stability by comparing them with estimators obtained from stratified 10-fold cross validation.

Mathematically, the jackknife value estimator is defined as

$$\hat{V}^{jk}(\hat{d}_n) = \frac{\sum_{i=1}^n U_i}{\sum_{i=1}^n W_i}$$

where $U_i = Y_i \frac{1\{A_i = \hat{d}_n^{(-i)}(\mathbf{X}_i)\}}{P(A_i|\mathbf{X}_i)}$, $W_i = \frac{1\{A_i = \hat{d}_n^{(-i)}(\mathbf{X}_i)\}}{P(A_i|\mathbf{X}_i)}$, $\hat{d}_n^{(-i)}$ is the decision rule estimated from a training set of size n with the i -th observation left out, and $P(A_i|\mathbf{X}_i)$ is the propensity score (see Supplemental Table 2 for definition of propensity score) of the testing set i -th

observation. Conceptually, $\hat{V}^{jk}(\hat{d}_n)$ is similar to $\hat{V}(d)$ with the decision rule estimated by the jackknife $\hat{d}_n^{(-i)}$. For our IDEA trial data, the propensity score is known and is simply the proportion of being in each of the three treatments since treatment and covariates are independent for randomized trials. For non-randomized studies, propensity scores need to be estimated by methods such as logistic regression. See Appendix A1 for definition of the estimated variance of the jackknife value estimator.

Model Selection. We performed a Z-test to compare the optimal PMM with the optimal ZOM. The test results are used to inform us of whether there is a strong precision medicine effect and whether or not ZOMs are always the optimal choice. Let $\hat{V}^{jk}(\hat{d}_{PMM})$ be the jackknife estimator of the value function of the selected optimal PMM and $\hat{V}^{jk}(\hat{d}_{ZOM})$ be the jackknife estimator of the value function of the optimal zero-order model. The null hypothesis was that there is no difference between the values of the selected optimal PM decision rule and the zero-order decision rule $H_0: V_0(\hat{d}_{PMM}) = V_0(\hat{d}_{ZOM})$ and the alternative hypothesis was two-sided $H_a: V_0(\hat{d}_{PMM}) \neq V_0(\hat{d}_{ZOM})$. With a significance level chosen to be 0.1, we conclude that there is evidence that the treatment rules derived from the optimal PMM provides statistically significant improvement in the outcome than the optimal ZOM if $p < 0.1$. See Appendix A2 for definition of the jackknife Z-test statistic.

Stratified Cross Validation. In addition to the jackknife method (i.e., LOOCV), we applied stratified 10-fold CV with 50 repetitions, with each fold stratified by the randomization group. Let $M = 50$ denote the total number of repetitions, $K = 10$ denote the number of CV folds, and $j = 1, \dots, KM$ denote all 500 folds regardless of the repetition. See Appendix A3 for definitions of estimated value function, its estimated variance, and the cross validation test statistics.

Similar test results were observed when we compared the optimal PMM with the optimal ZOM: For input data 1, the optimal PMM for weight loss since baseline was a list model with at most 2 nodes. Applied to future patients with the 10-fold CV method, the optimal rules derived from this list-based model would be expected to increase average weight loss to 10.8 kg at 18 months contrasted with 9.8 kg had all patient received D+E. The relative increment of 1.0 kg between the PMM and ZOM was significant ($p = 0.06$). For input data 2, the optimal PMM for IL-6 (log-transformed in the model) was list-based DTR with at most 2 nodes embedded with RF, which is one of the two optimal PM models the jackknife method detected in the Results section. Applied to future patients with the 10-fold CV method, the optimal rules derived from this list model would be expected to decrease average IL-6 level to 2.34 pg/mL compared with 2.56 pg/mL had all patients received D+E. The relative increment of 0.22 pg/mL was significant ($p = 0.09$). The CV estimated optimal rule for weight loss was the same as condition 1.1) in the Results section. The estimated optimal rule based on list DTR with a maximum of 2 nodes was the same as condition 2.1) in the Results section. Stratified 10-fold CVs tend to produce similar results as the jackknife method.

Multiple Outcomes. The coarse-to-fine grid search was defined as follows. First, a coarse grid search of weights between 0 and 1 with increment 0.1 was applied to find the

weight combinations (of length 3) that generate the top five lowest jackknife estimators of the value function, $\hat{V}^{jk}(\hat{d})$. Here, \hat{d} was trained by a random forests model and the \hat{V} 's were transformed to percentiles to be compared on the same scale across the three selected outcomes. Next, a fine grid search of increment 0.02 was conducted to a range within ± 0.06 of the five selected sets of weights to find the one weight combination that maximizes the lowest $\hat{V}^{jk}(\hat{d})$. This two-step grid search reduced computation time significantly, as opposed to one large fine grid search of weights between 0 and 1 with increment 0.02.

Consistency of Jackknife Estimators. Statistical inference properties of the jackknife estimators were evaluated through a mathematical proof and simulations. It is known that the estimate of expected prediction error calculated from cross validation is conditionally unbiased but its variance can be very large (21). Moreover, there have been theoretical arguments that claimed that it depends on how correlated the training data are and there are no universally unbiased estimator of such variance of expected prediction error under all distributions of observations (22). We argued that for our case jackknife estimates of value functions are asymptotically unbiased and their variances converge to zero as sample size increases. The consistency statement of a jackknife estimator was summarized in Theorem 1 provided with a proof (see Appendix B).

Generalizability. Our efforts in preventing overfitting and improving generalizability of our PM approach are represented three major ways: i) we applied feature selection with RF to reduce the complexity of input data; ii) we used the CV resampling technique to evaluate model performance as internal validation to all models; iii) we proposed a precision medicine-based approach for many of its advantages, one of which is that PM is carried under a causal framework which produces generalizable rules. For instance, basic causal assumptions (e.g., consistency, positivity, no unmeasured confounders) and the definition of value function estimators enable the conclusions to be applied to future population. Nonetheless, we recommend a follow-up to the IDEA trial or a new randomized clinical trial to be performed in the future to confirm our findings.

Simulation Analyses

In addition to the analyses on the IDEA data, we carried out extensive simulations to assess the performance of the jackknife estimators of value functions in various settings. We set up the simulations to mimic the IDEA data as closely as possible. The simulation results showed that i) precision medicine models (such as KRR) can provide good estimation of the true decision boundary (the true decision boundary is known for simulations but not for the real clinical data); ii) the jackknife estimator of the value function has a similar distribution to the best theoretical estimator of the value function; iii) the 95% confidence interval of our jackknife estimator has good coverage over the true value function around 95% of the time for high sample sizes; iv) the power of our Z-test between optimal PMM and optimal ZOM improves as sample size increases; v) the distribution of the proposed jackknife estimator is asymptotically normal. For specific details of how we conducted the simulations, please see Appendix C. We have provided simplified example R code of our precision medicine approach,

available on GitHub (<https://github.com/phoebejiang/pmoa>), for interested readers to download and implement our methods. Due to data privacy, we provided simulated data described in Appendix C as input data instead of the original IDEA data.

APPENDIX (Statistical Details)

A. Mathematical Definitions

A1. Definition of estimated variance of the jackknife value estimator: $\widehat{Var} \left[\hat{V}^{jk}(\hat{d}_n) \right]$.

Define $\bar{U}_n = \sum_{i=1}^n U_i$ and $\bar{W}_n = \sum_{i=1}^n W_i$. Let $R_i^{jk} = \frac{1}{\bar{W}_n} U_i - \frac{\bar{U}_n}{\bar{W}_n^2} W_i$ be an influence function-inspired form of value function, which is bias-corrected because $\sum_{i=1}^n R_i^{jk} = 0$ by definition. We defined the estimated variance of the jackknife value estimator as

$$\widehat{Var} \left[\hat{V}^{jk}(\hat{d}_n) \right] = \frac{1}{n(n-1)} \sum_{i=1}^n (R_i^{jk})^2.$$

We adjusted the summation by $n(n-1)$ because of $n-1$ degrees of freedom in the summation and correlation among the n training sets. The standard error of the value estimator is thus $\widehat{SE}(\hat{V}^{jk}) = \sqrt{\widehat{Var}(\hat{V}^{jk})}$.

A2. Definition of the Z-test statistic: $T^{jk}(\hat{d}_{PMM}, \hat{d}_{ZOM})$. The test statistic for the jackknife was a standardized difference between the two value estimates:

$$T^{jk}(\hat{d}_{PMM}, \hat{d}_{ZOM}) = \frac{\hat{V}^{jk}(\hat{d}_{PMM}) - \hat{V}^{jk}(\hat{d}_{ZOM})}{\sqrt{\frac{\sum_{i=1}^n (R_{PMM}^{jk} - R_{ZOM}^{jk})^2}{n(n-1)}}}.$$

The p-value for this test was defined as $p = 2 P(|T| \leq z) = 2 \int_{|T|}^{\infty} f(z) dz$ where $z \sim N(0,1)$. Note that the test statistic is expected to be nonnegative because the optimal PMM would either outperform the optimal ZOM or assign the same treatment to everyone as in the optimal ZOM.

A3. Definitions of the stratified cross validation estimated value function $\hat{V}^{cv}(\hat{d}_n)$, its estimated variance $\widehat{Var} \left[\hat{V}^{cv}(\hat{d}_n) \right]$, and the test statistics $T^{cv}(\hat{d}_{PMM}, \hat{d}_{ZOM})$. The estimated value function was defined as

$$\hat{V}^{cv}(\hat{d}_n) = \frac{\sum_{j=1}^{MK} \sum_{i=1}^{n_j} U_{ji}}{\sum_{j=1}^{MK} \sum_{i=1}^{n_j} W_{ji}}$$

where $i = 1, \dots, n_j$ is the i -th observation in the j -th overall fold, $U_{ji} =$

$Y_{ji} \frac{I(A_{ji} = \hat{d}_n^{(-j)}(X_{ji}))}{P(A_{ji}|X_{ji})}$, $W_{ji} = \frac{I(A_{ji} = \hat{d}_n^{(-j)}(X_{ji}))}{P(A_{ji}|X_{ji})}$, $\hat{d}_n^{(-j)}$ is the decision rule estimated from a training set of size n with the j -th fold left out, and $P(A_{ji}|X_{ji})$ is the propensity score

of the i -th observation in the j -th overall fold (known for randomized trials). We defined the estimated variance of the jackknife value estimator as

$$\widehat{Var}[\hat{V}^{cv}(\hat{d}_n)] = \frac{1}{K(MK - 1)} \sum_{j=1}^{MK} \sum_{i=1}^{n_j} (R_{ji}^{cv})^2$$

where $R_{ji}^{cv} = \frac{1}{\bar{W}_j} U_{ji} - \frac{\bar{U}_j}{\bar{W}_j^2} W_{ji}$ is an influence function-inspired form of the value function with $\bar{U}_j = \sum_{i=1}^{n_j} U_{ji}$ and $\bar{W}_j = \sum_{i=1}^{n_j} W_{ji}$ (similar to that defined in the jackknife method above and $\sum_{j=1}^{MK} \sum_{i=1}^{n_j} R_{ji}^{cv} = 0$). For CV, the variance estimate was adjusted by the degrees of freedom $MK - 1$ for MK overall folds as well as by the correlations among K folds for each repetition. The standard error of the value estimator is then $\widehat{SE}(\hat{V}^{cv}) = \sqrt{\widehat{Var}(\hat{V}^{cv})}$. Because the jackknife is a special case of CV, the value function estimates of the jackknife are also special cases of those of CV with $M = 1, K = n$. As we can see, the jackknife is simpler in terms of notation and computation for moderate n .

We applied the Z-test to stratified CV value estimates defined above with the test statistic adjusted by $K(MK - 1)$:

$$T^{cv}(\hat{d}_{PMM}, \hat{d}_{ZOM}) = \frac{\hat{V}^{cv}(\hat{d}_{PMM}) - \hat{V}^{cv}(\hat{d}_{ZOM})}{\sqrt{\frac{\sum_{j=1}^{MK} (R_{PMM,j}^{cv} - R_{ZOM,j}^{cv})^2}{K(MK-1)}}}$$

B. Theorem 1 and its proof. Theorem 1: Consistency of the jackknife estimator.

Assume

$$(A1) \mathbb{E}[P_X(\hat{d}_n(X) \neq \hat{d}_{n-1}(X))] \rightarrow 0,$$

$$(A2) \mathbb{E}\left[\frac{Y^2}{P^2(A|X)} + \frac{1}{P^2(A|X)}\right] < \infty.$$

Then

$$\frac{\sum_{i=1}^n \frac{Y_i 1\{A_i = \hat{d}_n^{(-i)}(X_i)\}}{P(A_i|X_i)}}{\sum_{i=1}^n \frac{1\{A_i = \hat{d}_n^{(-i)}(X_i)\}}{P(A_i|X_i)}} - \mathbb{E}[Y|A = \hat{d}_n(X)] \xrightarrow{p} 0$$

It is reasonable to assume (A1) because the training sets of size n and $n - 1$ are asymptotically equal, which implies that the decision functions estimated from these two training sets eventually converge as sample size grows to infinity. Assumption (A2) requires a finite second moment of the outcome adjusted by the propensity score and thus a finite variance of the adjusted outcome, which is easily satisfied for clinical data where the outcome itself is finite and is usually contained in a range. The second term in (A2) is automatically satisfied because propensity scores are bounded between 0 and 1, and it is used in the analogous proof of W_n . Given the two weak assumptions, Theorem 1 can be proved as follows.

Proof of Theorem 1.

Let $U_i = \frac{Y_i 1\{A_i = \hat{d}_n^{(-i)}(\mathbf{X}_i)\}}{P(A_i|\mathbf{X}_i)}$, $W_i = \frac{1\{A_i = \hat{d}_n^{(-i)}(\mathbf{X}_i)\}}{P(A_i|\mathbf{X}_i)}$, $U_n = n^{-1} \sum_{i=1}^n U_i$, and $W_n = n^{-1} \sum_{i=1}^n W_i$. First,

$$\mu_n = \mathbb{E}[U_n] = n^{-1} \sum_{i=1}^n \mathbb{E} \left[\frac{Y_i 1\{A_i = \hat{d}_n^{(-i)}(\mathbf{X}_i)\}}{P(A_i|\mathbf{X}_i)} \right] = \mathbb{E} \left[\frac{Y 1\{A = \hat{d}_{n-1}(\mathbf{X})\}}{P(A|\mathbf{X})} \right].$$

Denote $\tilde{\mu}_n = \mathbb{E} \left[\frac{Y 1\{A = \hat{d}_n(\mathbf{X})\}}{P(A|\mathbf{X})} \right]$, then

$$\begin{aligned} \mu_n - \tilde{\mu}_n &= \mathbb{E} \left[\frac{Y}{P(A|\mathbf{X})} (1\{A = \hat{d}_{n-1}(\mathbf{X})\} - 1\{A = \hat{d}_n(\mathbf{X})\}) \right] \\ &\leq M \mathbb{E} [1\{A = \hat{d}_{n-1}(\mathbf{X})\} - 1\{A = \hat{d}_n(\mathbf{X})\}] \\ &\quad + \mathbb{E} \left[\frac{|Y|}{P(A|\mathbf{X})} 1 \left\{ \frac{|Y|}{P(A|\mathbf{X})} > M \right\} \right] \rightarrow 0, \end{aligned}$$

where the convergence is based on (A1) for the first term in the inequality and (A2), which implies finite first moment, for the second term in the inequality. Given the first term in (A2), we have the following property of the variance

$$\begin{aligned} \text{Var}[U_n] &= n^{-1} \text{Var} \left[\sum_{i=1}^n U_i \right] = n^{-2} \sum_{i=1}^n \sum_{j=1}^n [\mathbb{E}(U_i U_j) - \mathbb{E}(U_i) \mathbb{E}(U_j)] \\ &= n^{-2} \sum_{i=1}^n \sum_{j=1}^n \left[\mathbb{E} \left(\frac{Y_i Y_j 1\{A_i = \hat{d}_n^{(-i)}(\mathbf{X}_i)\} 1\{A_j = \hat{d}_n^{(-j)}(\mathbf{X}_j)\}}{P(A_i|\mathbf{X}_i) P(A_j|\mathbf{X}_j)} \right) - \mu_n^2 \right] \\ &\rightarrow n^{-2} \sum_{i=1}^n \sum_{j=1}^n \left[\mathbb{E} \left(\frac{Y_i Y_j 1\{A_i = \hat{d}_n^{(-i,-j)}(\mathbf{X}_i)\} 1\{A_j = \hat{d}_n^{(-i,-j)}(\mathbf{X}_j)\}}{P(A_i|\mathbf{X}_i) P(A_j|\mathbf{X}_j)} \right) - \mu_n^2 \right] \\ &= n^{-2} \sum_{i=1}^n \sum_{j=1}^n \left\{ \left[\mathbb{E} \left(\frac{Y 1\{A = \hat{d}_{n-2}(\mathbf{X})\}}{P(A|\mathbf{X})} \right) \right]^2 - \mu_n^2 \right\} \\ &\rightarrow n^{-2} \sum_{i=1}^n \sum_{j=1}^n (\mu_n^2 - \mu_n^2) = 0, \end{aligned}$$

here both convergences are based on (A1). Thus, we have shown that

$$\begin{aligned} \mathbb{E}[U_n] - \tilde{\mu}_n &\rightarrow 0 \\ \text{Var}[U_n] &\rightarrow 0 \end{aligned}$$

Applying the same arguments as above to W_n with assumptions (A1) and the second term in (A2), we have

$$\begin{aligned}\tau_n &= \mathbb{E}[W_n] = \mathbb{E}\left[\frac{1\{A=\hat{d}_{n-1}(\mathbf{X})\}}{P(A|\mathbf{X})}\right], \\ \tilde{\tau}_n &= \mathbb{E}\left[\frac{1\{A=\hat{d}_n(\mathbf{X})\}}{P(A|\mathbf{X})}\right] = \mathbb{E}\left\{\mathbb{E}\left[\frac{1\{A=\hat{d}_n(\mathbf{X})\}}{P(A=\hat{d}_n(\mathbf{X})|\mathbf{X})}\middle|\mathbf{X}\right]\right\} = 1,\end{aligned}$$

and similarly

$$\begin{aligned}\mathbb{E}[W_n] - 1 &\rightarrow 0 \\ \text{Var}[W_n] &\rightarrow 0\end{aligned}$$

Thus, by the weak law of large numbers (WLLN),

$$U_n - \tilde{\mu}_n \xrightarrow{p} 0 \quad \text{and} \quad W_n - 1 \xrightarrow{p} 0,$$

which yields

$$\frac{U_n}{W_n} - \tilde{\mu}_n \xrightarrow{p} 0$$

by the multivariate continuous mapping theorem. This completes the proof because

$$\tilde{\mu}_n = \mathbb{E}\left[\frac{Y 1\{A=\hat{d}_n(\mathbf{X})\}}{P(A|\mathbf{X})}\right] = \mathbb{E}[Y \hat{d}_n(\mathbf{X})] = \mathbb{E}[Y|A=\hat{d}_n(\mathbf{X})]$$

This equation is derived by applying a version of Radon-Nikodym derivative (i.e. $dP^d/dP = 1\{a=d(\mathbf{x})\}/P(a|\mathbf{x})$ where P denotes the distribution of (\mathbf{X}, A, Y) and P^d denotes the distribution of (\mathbf{X}, A, Y) under the decision rule d (15)) and

$$\frac{\sum_{i=1}^n \frac{Y_i 1\{A_i=\hat{d}_n^{(-i)}(\mathbf{X}_i)\}}{P(A_i|\mathbf{X}_i)}}{\sum_{i=1}^n \frac{1\{A_i=\hat{d}_n^{(-i)}(\mathbf{X}_i)\}}{P(A_i|\mathbf{X}_i)}} - \mathbb{E}[Y|A=\hat{d}_n(\mathbf{X})] = \frac{U_n}{W_n} - \tilde{\mu}_n. \quad \square$$

C. Simulation Settings. For each observation, the simulation data can be written as a triplet (\mathbf{X}, A, Y) that consists of three clinical covariates $\mathbf{X} = \{X_1, X_2, X_3\}$ i.i.d. from uniform distribution $U(-2, 2)$, a treatment variable A of values $\{0, 1, 2\}$ generated from multinomial distribution $Multinom\left(\frac{1}{3}, \frac{1}{3}, \frac{1}{3}\right)$ independently of \mathbf{X} , and a response variable Y normally distributed with mean $Q_0 = X_1 + X_2 + \delta_0(\mathbf{X}, A)$ and standard deviation 1. We considered four scenarios with the following different choices of Q_0 :

- (1) $\delta_0(\mathbf{X}, A) = 1\{A > 0\}(1 - X_1^2 - X_2^2)(X_1^2 + X_2^2 - 3)^{1\{A=1\}}$
- (2) $\delta_0(\mathbf{X}, A) = 1\{A > 0\}(1\{X_2 \leq [X_1 - 2 \cdot 1\{A=2\}]\} - 1\{X_2 > [X_1 - 2 \cdot 1\{A=2\}]\})$
- (3) $\delta_0(\mathbf{X}, A) = 1\{A > 0\}(X_1 + X_2 - 1)(-X_1 - X_2 - 1)^{1\{A=1\}}$
- (4) $\delta_0(\mathbf{X}, A) = 1\{A > 0\}(X_2 - X_1^2)(X_1^2 - X_2 - 2)^{1\{A=1\}}$

Scenarios 1-4 were determined by X_1 and X_2 only, with X_3 as a nuisance variable. The true decision boundaries of these scenarios can be described as (1) two concentric circles, (2) two parallel sets of steps of length 1, (3) two parallel lines with slope 1, and

(4) two sets of parabolas (Supplemental Figure 2). The purpose of including various scenarios in this simulation study is to explore whether candidate models can work well with simple and difficult boundary structures. Samples sizes were chosen to be 50, 100, 200, 400, which cover our clinical data sample sizes, and 100 simulations were performed for each sample size. The estimated decision rule was denoted as \hat{d}_n where n is the training size, and an independent and identically distributed (i.i.d.) sample of the same size as the simulation data (X, A, Y) was denoted as $(\tilde{X}, \tilde{A}, \tilde{Y})$. We derived four estimators on simulation data:

1) Empirical estimator, where the same n observations were used for training and testing the decision rule.

$$\hat{V}_1(\hat{d}_n) = \frac{\sum_{i=1}^n Y_i \mathbf{1}\{A_i = \hat{d}_n(X_i)\} / P(A_i | X_i)}{\sum_{i=1}^n \mathbf{1}\{A_i = \hat{d}_n(X_i)\} / P(A_i | X_i)}$$

2) Jackknife estimator, where $n - 1$ observations were used for training the decision rule and the n -th observation for testing.

$$\hat{V}_2(\hat{d}_n) = \frac{\sum_{i=1}^n Y_i \mathbf{1}\{A_i = \hat{d}_n^{(-i)}(X_i)\} / P(A_i | X_i)}{\sum_{i=1}^n \mathbf{1}\{A_i = \hat{d}_n^{(-i)}(X_i)\} / P(A_i | X_i)}$$

3) Jackknife + test estimator, where $n - 1$ observations were used for training and an independent and identically distributed copy of one observation was used for testing.

$$\hat{V}_3(\hat{d}_n) = \frac{\sum_{i=1}^n \tilde{Y}_i \mathbf{1}\{\tilde{A}_i = \hat{d}_n^{(-i)}(\tilde{X}_i)\} / P(\tilde{A}_i | \tilde{X}_i)}{\sum_{i=1}^n \mathbf{1}\{\tilde{A}_i = \hat{d}_n^{(-i)}(\tilde{X}_i)\} / P(\tilde{A}_i | \tilde{X}_i)}$$

4) Empirical + test estimator, where all n observations were used for training and an independent and identically distributed copy of the training data with the same size n was used for testing.

$$\hat{V}_4(\hat{d}_n) = \frac{\sum_{i=1}^n \tilde{Y}_i \mathbf{1}\{\tilde{A}_i = \hat{d}_n(\tilde{X}_i)\} / P(\tilde{A}_i | \tilde{X}_i)}{\sum_{i=1}^n \mathbf{1}\{\tilde{A}_i = \hat{d}_n(\tilde{X}_i)\} / P(\tilde{A}_i | \tilde{X}_i)}$$

5) Empirically true estimator, where all n observations were used for training and an independent copy of the training data of size $n_{pop} = 1,000,000$ was used for testing.

$$V_o(\hat{d}_n) = \frac{\sum_{i=1}^{n_{pop}} \tilde{Y}_i \mathbf{1}\{\tilde{A}_i = \hat{d}_n(\tilde{X}_i)\} / P(\tilde{A}_i | \tilde{X}_i)}{\sum_{i=1}^{n_{pop}} \mathbf{1}\{\tilde{A}_i = \hat{d}_n(\tilde{X}_i)\} / P(\tilde{A}_i | \tilde{X}_i)}$$

The jackknife estimator \hat{V}_2 was applied in the knee OA study described in the main paper. In these simulations, we focused on the other three estimators for comparison. Estimator \hat{V}_1 was not honest (i.e., ‘honesty’ means that data are used for training or testing but not both) and was expected to overfit the training set. Estimator \hat{V}_3 was considered as a bridge between \hat{V}_2 and \hat{V}_4 because it was tested on independent copies like \hat{V}_4 but trained based on the jackknife method like \hat{V}_2 . We hoped to find that \hat{V}_2 has similar performance and statistical inferences as \hat{V}_4 , which is

the honest estimator with the largest training set. In comparison, estimator V_o was trained on the same training set of size n as the empirical estimator but tested on a simulated data set of a much larger test size that generated the best possible estimates of the truth one can obtain empirically.

Similar to the IDEA trial analysis, we fit the three ZOMs and 23 PMMs (excluding M6) to the simulation data, with two main changes to the precision medicine models: i) multiple outcome RF model (M6 in Table 2) was not possible for data with one outcome hence we applied only 23 PMMs for simulations, and ii) for RLT and RF models, the default number of variables randomly sampled at each split as candidates was one for four covariates (three X 's and one A) and we forced it to be two so the model is not forced to split on the only one candidate variable. We also examined the distribution of four estimators of value functions together with the empirically true estimates and compared the optimal PMM and optimal ZOM with a Z-test. The test statistic for each simulation is

$$T^{sim}(\hat{d}_{PMM}, \hat{d}_{ZOM}) = \frac{\hat{V}(\hat{d}_{PMM}) - \hat{V}(\hat{d}_{ZOM})}{\sqrt{\frac{\sum_{i=1}^n (R_{PMM,i} - R_{ZOM,i})^2}{n(n-1)}}$$

where \hat{d}_{PMM} and \hat{d}_{ZOM} are estimated decision rules for the optimal PMM and the optimal ZOM respectively, \hat{V} stands for estimated value function, and $R_{PMM,i}$ and $R_{ZOM,i}$ represent the bias-corrected, influence function-inspired value function of the i -th individual under the rule for the optimal PMM and ZOM respectively. The null hypothesis was that the future reward of the optimal PMM rule is as much as the optimal ZOM rule.

We also examined the asymptotic normality property of jackknife estimators via simulations. For each sample size and data scenario across 100 simulations, we calculated the following test statistic:

$$T_o^{sim} = \frac{[\hat{V}^{jk}(\hat{d}_{PMM}) - \hat{V}^{jk}(\hat{d}_{ZOM})] - [V_o(\hat{d}_{PMM}) - V_o(\hat{d}_{ZOM})]}{\sqrt{\frac{\sum_{i=1}^n (R_{PMM,i}^{jk} - R_{ZOM,i}^{jk})^2}{n(n-1)}}$$

which is a function of jackknife estimators and a “shifted” version of T^{sim} . The test statistic measures the difference between the estimated value function of optimal PMM and that of optimal ZOM, shifted by the corresponding difference in the true value function.

Simulation Results. First, we looked at the accuracy of the precision medicine models for reproducing the true decision boundaries of the four scenarios (Supplemental Figure 3). KRR was again selected because it represents a precision medicine model with good performance in different scenarios. The estimated decision boundaries were based on fitting the model once for a simulation sample size of $n = 500$. It is clear that KRR was able to estimate the decision boundary of scenarios 1, 3,

and 4, with scenario 3 being the best. It had a difficulty finding the second set of steps for scenario 2 due to the small decision area of treatment $A = 2$ but was able to detect the longer set of steps.

Second, we compared the distribution of our jackknife estimators \hat{V}_2 with the distribution of empirical + test estimators \hat{V}_4 , which are the best possible estimators but not feasible in reality because we often do not have an independent copy of the sample data with the same size (or we cannot afford 50/50 splitting of our available data). Supplemental Figure 4 contains Q-Q plots that compare four estimators \hat{V}_1 to \hat{V}_4 with the empirical + test estimator \hat{V}_4 based on the KRR model, which had overall good performance compared with other models. The purple curve is a straight line because it is a comparison between \hat{V}_4 and itself. The green curve, our jackknife estimator, mostly follows the straight line except at the left tail (i.e. when the estimators are less than -2) for difficult scenarios such as 1 and 4. As sample size increases the green curve becomes straighter for all scenarios. This indicates that our jackknife estimators have a similar distribution as the empirical + test estimators, especially for higher sample sizes.

We then explored the coverage of the jackknife estimators \hat{V}_2 over V_o . Given \hat{V}_2 and its standard error, a 95% confidence interval (CI) was calculated for each simulation, $\hat{V}_2 \pm z_{0.975} \cdot SE(\hat{V}_2)$, where $z_{0.975} \approx 1.96$ is the standard normal quantile of 97.5%. The coverage was defined as the proportion of simulations whose 95% CI contains V_o , which has a Monte Carlo error (the maximum standard error of the estimated proportion) of 5%. We still used KRR as an example of a good performing PMM and summarized the percentage of coverage with 95% CIs in Supplemental Table 3. Overall, coverage generally increases as sample size goes up (Supplemental Table 3). Scenarios 2-4 have at least or almost 95% coverage for higher sample sizes. Scenario 1 did not reach as high a coverage as the other scenarios across sample sizes; we believe this is because concentric circles are complex, non-linear decision boundaries. After increasing the sample size to 800, we saw a 96% coverage for scenario 1 and concluded that the 92%-to-88% dip at $n = 400$ was due to Monte Carlo errors. With more simulations, we were able to see more uniform patterns.

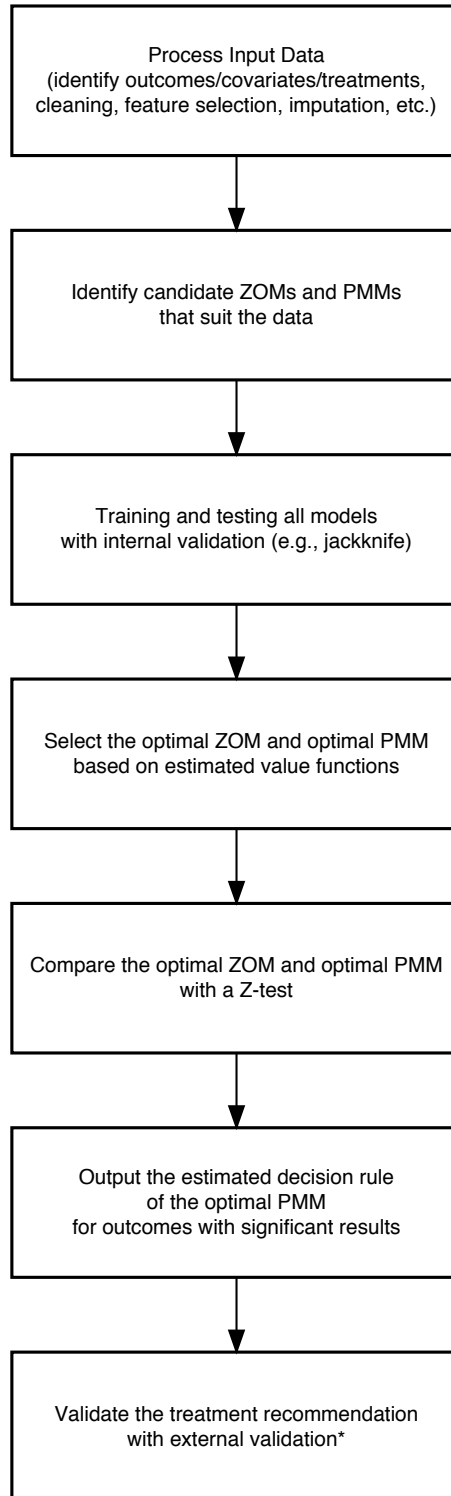
Next, we estimated the power of the jackknife test statistic T_0^{sim} . Here, power was estimated by the proportion of simulations whose p-values were under 0.05 out of 100 simulations, which also has a Monte Carlo error of 5%. This reflects how often the test will detect a significant effect of optimal PMM over optimal ZOM when there is an effect. We found that T_0^{sim} experienced difficulty at small sample sizes and at large sample sizes for complex boundaries such as scenarios 1 and 2. Yet, the estimated power almost always increased as sample size increased for each scenario (Supplemental Table 4). Scenario 3, the decision boundary for which KRR had good accuracy in the previous prediction setting, reached the highest power (81%) at $n = 400$ compared with other scenarios. Given how power tends to increase with larger sample sizes, a similar trend to CI coverage in Supplemental Table 3, we would expect to see higher power for the jackknife test statistic had there been larger sample sizes.

Lastly, we studied the normality of jackknife estimators by comparing the distribution of T_o^{sim} over 100 simulations with the standard normal distribution. The comparison was visualized via Q-Q plots for all four scenarios (Supplemental Figure 5). Only two sample sizes, 50 and 400, were shown for cleaner plots. We can see that the distribution of test statistic is mostly standard normal in the middle and the scattering of points in Scenarios 2 and 3 is particularly close to a straight line. In addition to visual inspections, we also tested the normality of T_o^{sim} using the Shapiro-Wilk test. Simulation studies have shown that Shapiro-Wilk (SW) test has good power properties over symmetric distributions as well as a wide range of skewed distributions (23). Based on both the Q-Q plots (Supplemental Figure 5) and SW test results (Supplemental Table 5), T_o^{sim} has fewer outliers and is more normally distributed (especially in the middle) when sample size increases. We were only able to reject the null hypothesis that T_o^{sim} follows a standard normal distribution for scenarios 3 and 4, which we believe was due to a few outliers at the positive end. In summary, we concluded that there is not enough evidence to reject the hypothesis that T_o^{sim} is standard normally distributed for moderate to high sample sizes ($n \geq 100$) in all four decision boundary scenarios, and the Q-Q plots indicated evidence for asymptotic normality. In addition to the consistency and asymptotic normality properties inspected here, there are more complex and technically rigorous approaches to value function inference than what we propose here: for a review of such methods, see (24).

REFERENCES

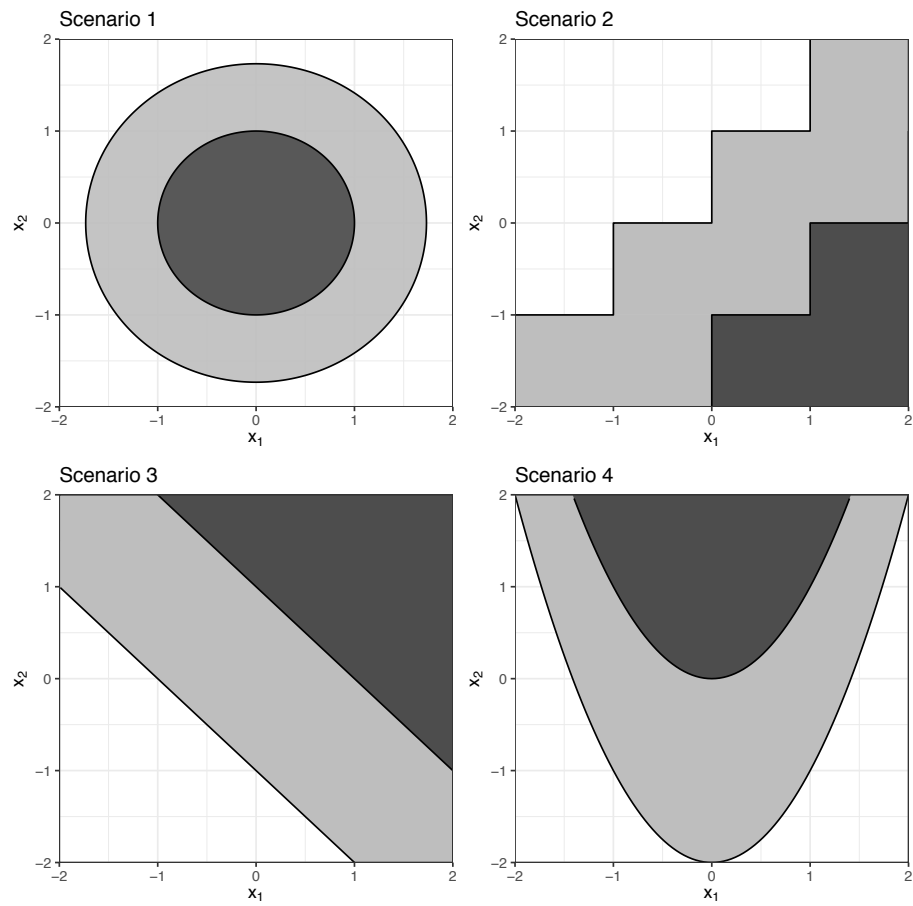
1. Stekhoven DJ, Bühlmann P. MissForest--non-parametric missing value imputation for mixed-type data. *Bioinformatics* 2012;28:112–118.
2. Paterek A. Improving regularized singular value decomposition for collaborative filtering. *Proceedings of KDD cup and workshop* 2007;2007:5.
3. Zhu R, Zeng D, Kosorok MR. Reinforcement Learning Trees. *J Am Stat Assoc* 2015;110:1770–1784.
4. Zhang Y, Laber EB, Davidian M, Tsiatis AA. Estimation of optimal treatment regimes using lists. *J Am Stat Assoc* 2017:0–0.
5. Laan MJ van der, Polley EC, Hubbard AE. Super learner. *Stat Appl Genet Mol Biol* 2007;6:Article25.
6. “Super Learner In Prediction” by Eric C. Polley and Mark J. van der Laan. Available at: <https://biostats.bepress.com/ucbbiostat/paper266/>. Accessed August 21, 2019.
7. Computational Statistics, by G. H. Givens and J. A. Hoeting. Available at: <https://www.stat.colostate.edu/computationalstatistics/>. Accessed August 26, 2019.
8. Zhou X, Mayer-Hamblett N, Khan U, Kosorok MR. Residual weighted learning for estimating individualized treatment rules. *J Am Stat Assoc* 2017;112:169–187.
9. Zhao Y, Zeng D, Rush AJ, Kosorok MR. Estimating individualized treatment rules using outcome weighted learning. *J Am Stat Assoc* 2012;107:1106–1118.
10. Chipman HA, George EI, McCulloch RE. BART: Bayesian Additive Regression Trees. *Ann Appl Stat* 2010;4:266–298.

11. Friedman J, Hastie T, Tibshirani R. Regularization Paths for Generalized Linear Models via Coordinate Descent. *J Stat Softw* 2010;33:1–22.
12. Liaw A, Wiener M. Classification and regression by randomForest. *R news* 2002;2:18–22.
13. Holloway ST, Laber EB, Linn KA, Zhang B, Davidian M, Tsiatis AA. *DynTxRegime: Methods for Estimating Optimal Dynamic Treatment Regimes*. R package; 2018.
14. Sparapani RA, Logan BR, McCulloch RE, Laud PW. Nonparametric survival analysis using Bayesian Additive Regression Trees (BART). *Stat Med* 2016;35:2741–2753.
15. Qian M, Murphy SA. Performance guarantees for individualized treatment rules. *Ann Stat* 2011;39:1180–1210.
16. Quenouille MH. Approximate tests of correlation in time-series 3. *Math Proc Camb Phil Soc* 1949;45:483.
17. Tukey J. Bias and confidence in not quite large samples. *Ann Math Statist* 1958;29.
18. Kohavi R. A study of cross-validation and bootstrap for accuracy estimation and model selection. *Ijcai* 1995;14:1137.
19. Burman P. A Comparative Study of Ordinary Cross-Validation, v-Fold Cross-Validation and the Repeated Learning-Testing Methods. *Biometrika* 1989;76:503.
20. Zhang Y, Yang Y. Cross-validation for selecting a model selection procedure. *J Econom* 2015;187:95–112.
21. Breiman L. Heuristics of instability and stabilization in model selection. *Ann Statist* 1996;24:2350–2383.
22. Bengio Y, Grandvalet Y. No Unbiased Estimator of the Variance of K-Fold Cross-Validation. *Journal of Machine Learning Research* 2004.
23. Yap BW, Sim CH. Comparisons of various types of normality tests. *J Stat Comput Simul* 2011;81:2141–2155.
24. Laber EB, Lizotte DJ, Qian M, Pelham WE, Murphy SA. Dynamic treatment regimes: technical challenges and applications. *Electron J Stat* 2014;8:1225–1272

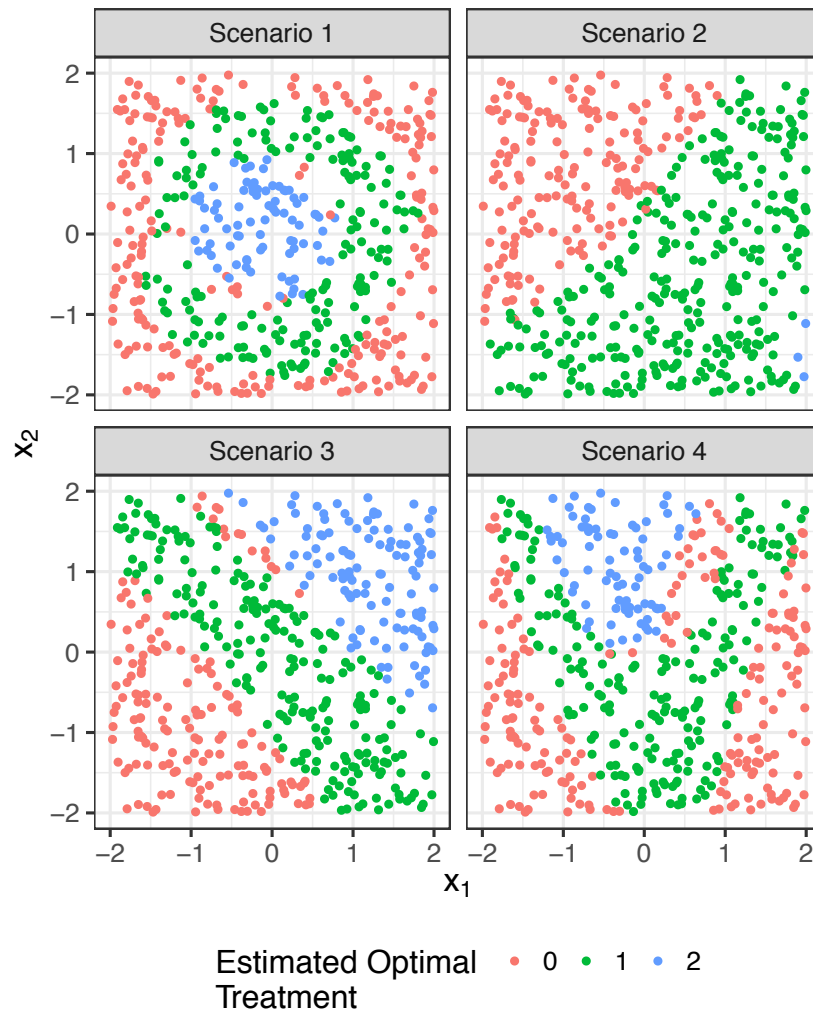


Supplemental Figure 1. Flowchart of the proposed precision medicine approach. An asterisk means the step was not performed in this analysis due to unavailable data but is highly recommended for a more complete analysis.

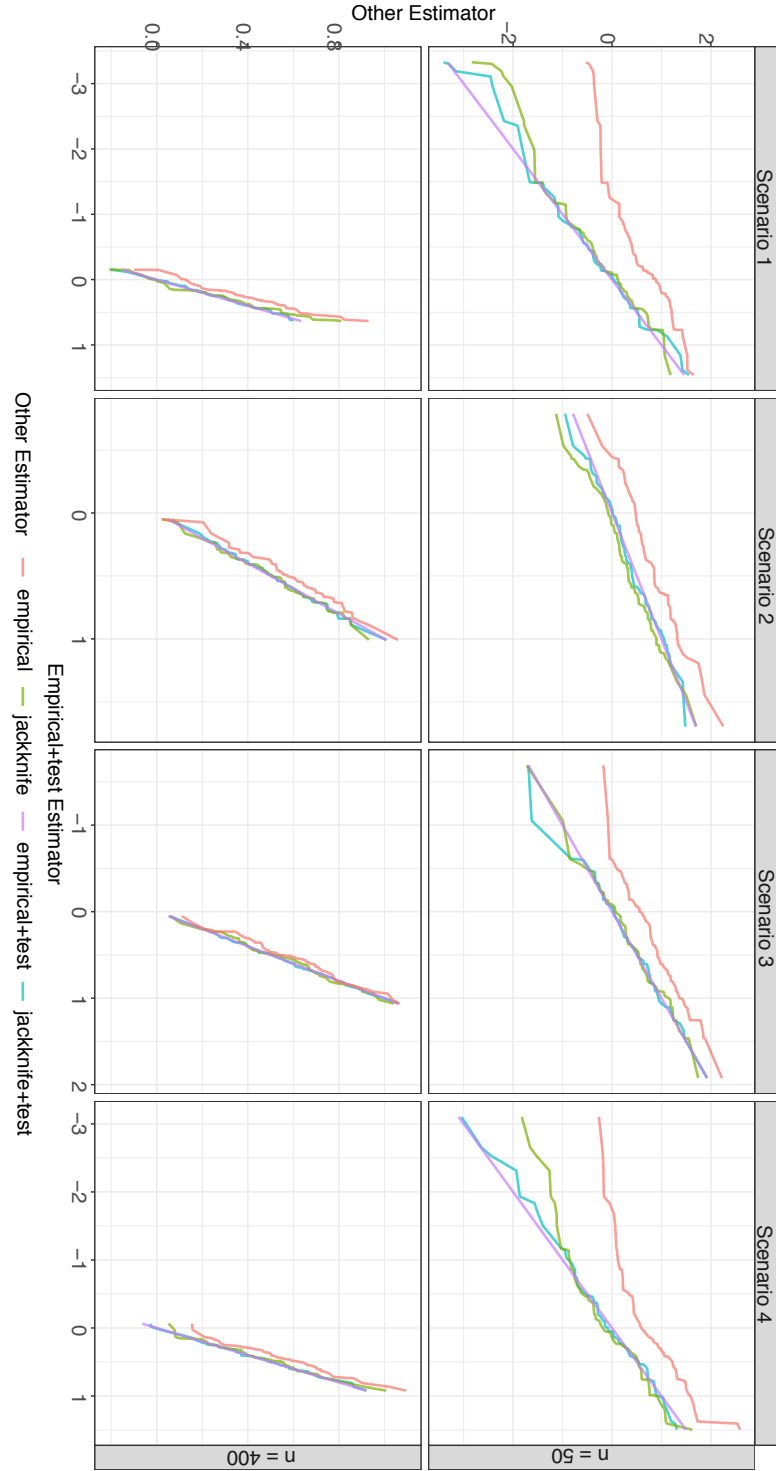
Supplemental Figure 2. True decision boundaries of simulation scenarios (where white, light gray, and dark gray areas represent true optimal treatment 0, 1, and 2 respectively)



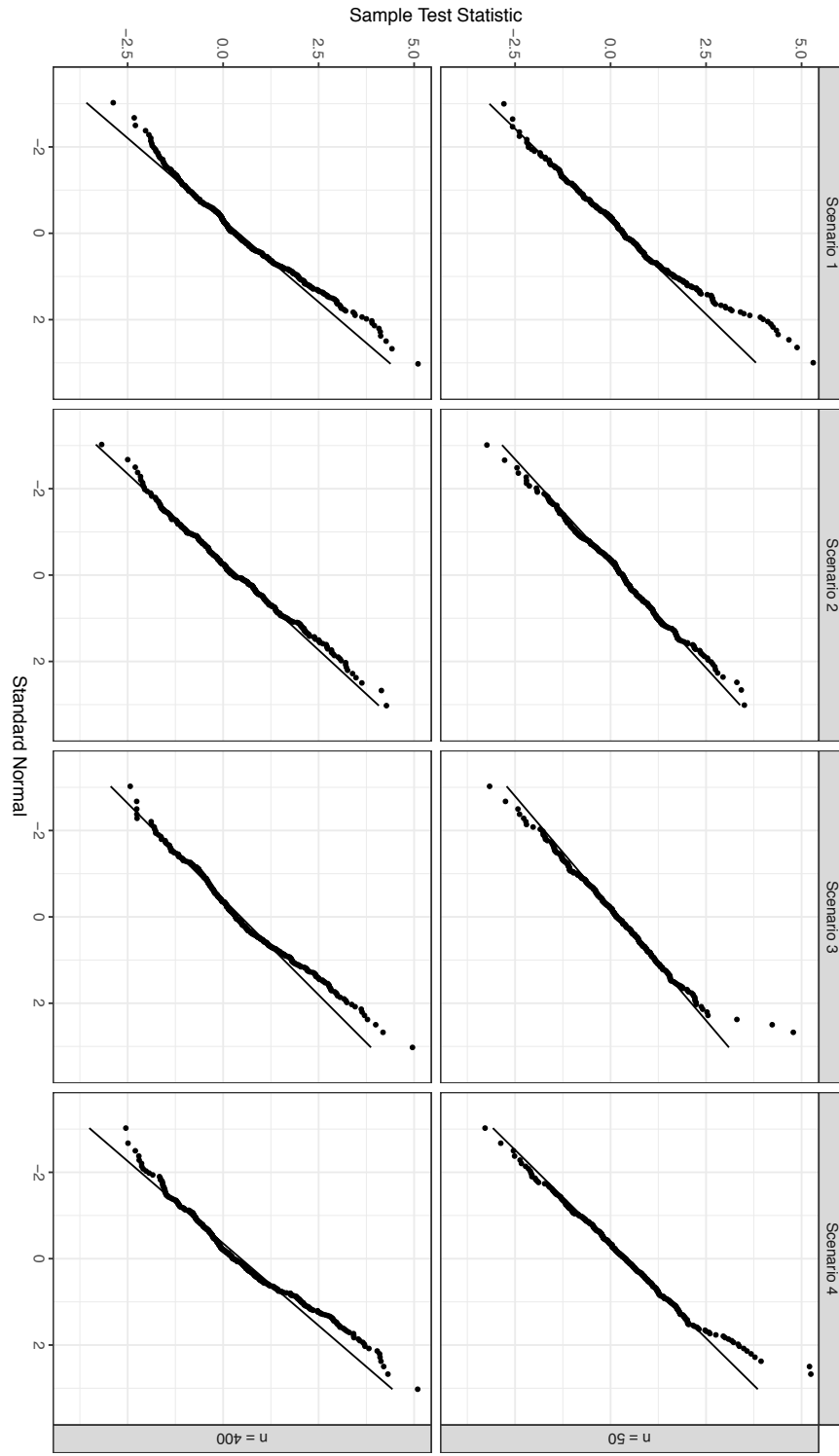
Supplemental Figure 3. Estimated decision boundaries for a simulated dataset of size $n = 500$ trained by KRR models (scenario 1 - circles, scenario 2 - steps, scenario 3 – lines, scenario 4 – quadratic curves)



Supplemental Figure 4. Q-Q plots of the distribution of estimators \hat{V}_1 to \hat{V}_4 versus the distribution of \hat{V}_4 based on the KRR model across 100 simulations for $n = 50$ and $n = 400$ over 4 scenarios (colors: empirical is red, jackknife is green, empirical+test is purple, jackknife+test is blue).



Supplemental Figure 5. Q-Q plots of the distribution of jackknife T_o^{sim} versus the standard normal distribution across 100 simulations for $n = 50$ and $n = 400$ over 4 scenarios



Supplemental Table 1. Listing of statistical terminology and abbreviations (used in the main paper)

Term	Abbr.	Brief Definition
Cross Validation	CV	A validation technique that reduces bias and checks for generalizability of model results beyond the specific data used to fit the model.
Decision Tree		A decision model with a shape like an upside-down tree where prediction or classification can be made through the model's hierarchical flowchart-like structure.
Dimension Reduction		A group of approaches that describes the important characteristics of data using a smaller set of variables (or a smaller set of some variations of variables).
Dynamic Treatment Regime	DTR	The individualized treatment rules that recommend effective and adaptive treatment plans for individuals where dynamic refers to variations in the covariates, not necessarily over time.
Individualized Treatment Rule	ITR	A function that maps patient characteristics to an intervention, thus recommending treatments based on individualized characteristics.
Jackknife	JK	A cross validation method where every individual takes turns to test the performance and generalization of the model trained on the remaining (n-1) individuals in the data. More in supplemental materials.
Leave-one-out Cross Validation	LOOCV	Also known as n -fold cross validation and jackknife. See Jackknife for definition.
Machine Learning	ML	A field of study consisting of statistical and computational tools that learn patterns and representations from data without strong underlying assumptions on the data generating mechanism. Often used in high-dimensional settings where traditional statistical models tend to fail.
Minimax		A procedure that makes decisions based on minimizing the highest loss or maximizing the lowest gain.
Optimal Treatment Rule		The individualized treatment rule that informs which individuals would benefit the most (assuming higher outcomes are favorable) from a given intervention, among all other possible individualized treatment rules.
Precision Medicine	PM	A data-driven approach that optimizes clinical outcomes while tailoring treatment recommendations to patient heterogeneity.
Precision Medicine Model	PMM	A machine learning model that uses advanced, precision medicine-based approaches to estimate individualized treatment rules.

Random Forests	RF	An ensemble tree-based method that make prediction (for continuous variables) and classification (for categorical variables) by aggregating many individual decision trees while providing variable importance scores that are often used to select important variables.
Value Function	V	A scalar measure of performance for each individualized treatment rule that evaluates the expectation of an outcome had future patients followed the estimated decision rule that is derived from training input data. Higher value functions are desirable given higher outcomes are desirable. More in supplemental materials.
Zero-Order Model	ZOM	A simple model that assigns the same treatment to all individuals as the treatment rule. Named after zero order processes, which are fixed decision rules that do not change by individual.

Supplemental Table 2. Listing of statistical terminology and abbreviations (used in the supplemental material)

Term	Abbr.	Brief Definition
Bayesian Additive Regression Tree	BART	An ensemble method that combines Bayesian regression trees to make predictions or classifications.
Coverage (of a confidence interval)		The proportion of simulations whose confidence interval estimation contains the true value of interest.
Gaussian Kernel		A kernel function based on the Gaussian density function.
Honesty		The situation where data are used for training or testing but never both, often preferred to avoid overfitting.
Imputation		A statistical process that substitutes missing data with values predicted from the observed data to make the dataset complete.
Influence Function		A measure of how much a change in the observed data influences the estimator, often used to study model robustness and variability.
Kernel Function		A computationally cheaper method to convert a non-linear problem to a linear learning problem. Often used inside a decision rule.
Kernel Ridge Regression	KRR	A ridge regression model that directly computes kernel functions to make predictions.
List-based Dynamic Treatment Regime	List-based DTR	An interpretable precision medicine model that estimate optimal treatment regimens with a sequence of decision rules which can be interpreted as a set of “if-then” statements.
Monte Carlo Error		The maximum standard error of an estimated proportion.
Multiple Imputation by Chained Equations	MICE	An imputation method that uses flexible chained equations to generate multiple copies of imputed datasets, accounting for the uncertainty in the imputations.
Outcome Weighted Learning	OWL	A precision medicine model that learns the optimal treatment regimen by optimizing clinical outcomes directly as a weighted classification problem, as opposed to a two-step plug-in regression problem.
Out-of-bag Error	OOB	For resampling methods such as random forests, out-of-bag error measures the overall prediction error without the need for an independent validation set. It is calculated by averaging each individual’s prediction error on trees that do not contain the individual in the bootstrap sample.

Penalized Regression		A linear regression model that penalizes high-dimensional data in the model by shrinking the coefficients. Well-known penalized regression models include LASSO and ridge.
Penalty		An additional term in regression models that penalizes large values of model coefficients, favoring less complex models and balancing bias-variance tradeoff.
Propensity Score	PS	The probability of receiving a treatment conditioning on the observed X-variables, often used to provide balance for the number of subjects receiving each treatment.
Q-Q Plot		The quantile-quantile plot displays quantiles of two groups of data and compares their probability distributions. The more similar the two distributions are, the closer the points are to the 45 degree straight line ($y = x$).
Reinforcement Learning Tree	RLT	An extension combining random forests and reinforcement learning that selects variables that improve outcomes in the long run, as opposed to the immediate future.
Residual Weighted Learning	RWL	An extension of outcome weighted learning that uses outcome residuals instead of the original outcomes to handle various types of outcomes (continuous, count, categorical) and any shifts in the outcomes.
Super Learning	SL	An ensemble machine learning method that takes a weighted average of the base learners instead of selecting one best learner as the optimal treatment regime.

Supplemental Table 3. Coverage of the empirically true estimator V_o with 95% CI of \hat{V}_2

Sample Size	50	100	200	400
Scenario 1	84%	87%	92%	88%
Scenario 2	91%	91%	96%	96%
Scenario 3	93%	97%	96%	96%
Scenario 4	89%	88%	90%	94%

Supplemental Table 4. Estimated power of jackknife T_0^{sim} based on 100 simulations

Sample Size	50	100	200	400
Scenario 1	13%	7%	18%	38%
Scenario 2	16%	13%	23%	34%
Scenario 3	15%	24%	41%	81%
Scenario 4	11%	15%	35%	56%

Supplemental Table 5. P-values of Shapiro-Wilk test of normality on jackknife T_0^{sim}

Sample Size	50	100	200	400
Scenario 1	0.20	0.37	0.15	0.18
Scenario 2	0.85	0.92	0.41	0.79
Scenario 3	< 0.01	0.99	0.13	0.61
Scenario 4	< 0.01	0.67	0.81	0.84